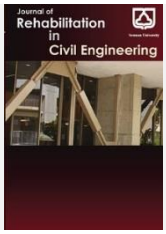

Journal of Rehabilitation in Civil Engineering

Journal homepage: https://civiljournal.semnan.ac.ir/

Deterministic and Probabilistic Seismic Hazard Analysis of Kunduz Airport (Afghanistan)

Mohammad Jawad Rahimi [1]; Abdulhai Kaiwaan [2]; Shamsullah Anwari [3]; Sayed Javid Azimi [4]; Zaher Rezaie [5,6*]

1. Ph.D. Student, Department of Structural Engineering, Afghan International Islamic University, Kabul, Afghanistan
2. Ph.D., Department of Structural Engineering, Afghan International Islamic University, Kabul, Afghanistan
3. Head of the Civil Engineering Department, Faculty of Engineering, Badakhshan University, Kabul, Afghanistan
4. Ph.D., Department of Structural Engineering, Afghan International Islamic University, Kabul, Afghanistan
5. Lecturer, Department of Civil Engineering, Kateb University, Kabul, Afghanistan
6. Ph.D. Student, Department of Civil Engineering, Ferdowsi University of Mashhad, Mashhad, Iran

* Corresponding author: *zaher.rezaie@kateb.edu.af*

ARTICLE INFO

Article history:
Received: 24 May 2025
Revised: 02 August 2025
Accepted: 17 August 2025

Keywords:
Seismic hazard analysis;
Kunduz Airport;
Deterministic approach;
Probabilistic approach;
Peak ground acceleration;
Seismic risk mitigation.

ABSTRACT

This study presents the first site-specific seismic hazard assessment of Kunduz Airport, a critical infrastructure located in the seismically active Alpine–Himalayan belt of northeastern Afghanistan. Both deterministic seismic hazard analysis (DSHA) and probabilistic seismic hazard analysis (PSHA) are employed to estimate peak ground acceleration (PGA), incorporating historical and instrumental seismicity data, regional tectonic frameworks, and local soil conditions (Vs30 = 250–300 m/s). The analysis utilizes regionally calibrated ground motion prediction equations (GMPEs) from the NGA-West2 suite within a logic-tree framework to account for epistemic uncertainties. The PSHA results yield a median PGA of 0.411g for a 2% probability of exceedance in 50 years (return period ~2475 years), while the DSHA indicates a maximum PGA of 0.41g, primarily governed by the Chaman fault. The Central Badakhshan and Takhar faults are also identified as major seismic sources contributing to site hazard. A comparative evaluation of international seismic design codes (Iranian Standard 2800, ASCE 7-16, Eurocode 8) reveals notable discrepancies in spectral acceleration and base shear values, emphasizing the necessity of local code calibration for performance-based design (PBD) of essential facilities in Afghanistan. Unlike previous regional studies such as Bakhshi et al. (2025), this research incorporates updated GMPE logic trees, nonlinear soil classification, and direct code-spectrum comparisons, offering a robust and localized hazard framework. The results contribute to seismic code development and risk mitigation planning for vital transportation infrastructure in Afghanistan.

E-ISSN: 2345-4423

How to cite this article:
Rahimi, M. J., Kaiwaan, A., Anwari, S., Azimi, S. J. and Rezaie, Z. (2026). Deterministic and Probabilistic Seismic Hazard Analysis of Kunduz Airport (Afghanistan). Journal of Rehabilitation in Civil Engineering, 14(2), 2354. https://doi.org/10.22075/jrce.2025.2354

1. Introduction

Throughout history, the mitigation of natural hazards, particularly earthquakes, has been a critical human concern due to their devastating impact on life and infrastructure. A fundamental step in addressing this risk is a thorough understanding of earthquake characteristics through seismic hazard analysis. This analysis employs methodologies to predict the effects of future earthquakes, primarily focusing on ground motion parameters. Evolving from reliance on earthquake intensity due to historical limitations in measurement tools, modern seismic hazard analysis is now indispensable for earthquake-resistant structural design, seismic risk assessment, loss estimation, insurance, and the development of crucial seismic zoning maps for standard and critical infrastructure, including dams and nuclear power plants.

Seismic hazard analysis quantitatively estimates ground motion risks at specific sites by considering factors such as distance to potential seismic sources, earthquake magnitude, attenuation relationships, and local soil conditions. Earthquakes are fundamentally linked to the rupture of geological faults caused by the gradual accumulation of stress from tectonic plate movements, thereby necessitating the integration of seismic, geological, and tectonic data for accurate hazard assessment. The spatial distribution of active faults within 200 km of Kunduz city is illustrated in Figure 1 [1]. Identifying seismotectonic provinces, based on the synthesis of this data (Figure 2 provides a seismic map of Afghanistan [2]), allows for the delineation of regions with distinct seismic behavior. The cornerstone of this analysis lies in the careful selection of seismic and tectonic datasets, including the identification and characterization of active faults, defined as those exhibiting activity within the last 11,000 years. Statistical methods are crucial for estimating the probability of future earthquakes of specific magnitudes, requiring the systematic classification, organization, and probabilistic modeling of historical earthquake data. This study provides the first site-specific seismic hazard analysis for an airport in Afghanistan using NGA-West2 models and a logic-tree framework. It also introduces localized code comparisons and soil-based Vs30 adjustments, which have not been previously applied in Afghan seismic research.

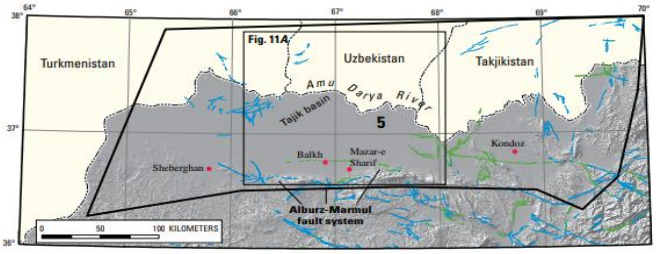

Fig. 1. Active faults within 200 km from the city of Kunduz [1].

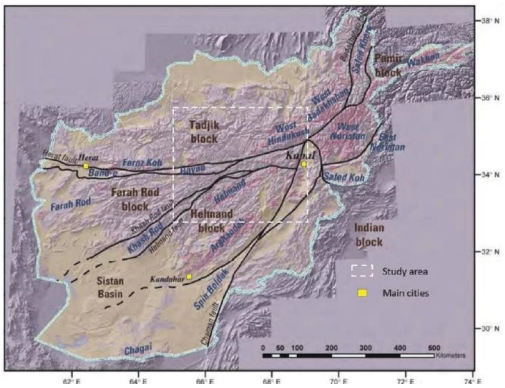

Fig. 2. Seismic map of Afghanistan [2].

Given its geographical location within the highly active Alpine-Himalayan seismic belt, Kunduz Airport in Afghanistan faces a significant vulnerability to seismic hazards. Strikingly, no dedicated seismic hazard analysis has been conducted for any airport in Afghanistan to date, despite their paramount role in

transportation and emergency response. Kunduz Airport, a key aviation hub in the northeastern part of the country, is situated in close proximity to major active faults (as shown in Figure 1), including the Central Badakhshan Fault and the Takhar Fault, thereby amplifying its susceptibility to seismic threats.

Recent studies have significantly advanced our understanding of seismic hazard assessment methodologies across various regions.While Bakhshi et al. (2025) presented regional estimates for Kunduz, this study offers a site-specific seismic hazard assessment at Kunduz Airport using updated logic-tree methodology, customized GMPEs, and local Vs30-based adjustments [3]. Complementary research by Yucemen (2005) in Turkey demonstrated innovative applications of probabilistic analysis by integrating seismic risk assessments with financial models to determine appropriate insurance premiums for earthquake-prone areas [4]. In China's Luding region, Bai et al. (2024) provided valuable empirical evidence through site investigations examining the effectiveness of seismic isolation techniques for earthquake damage mitigation [5]. The Kabul Basin's seismic risks were thoroughly investigated by Shnizai et al. (2023), whose fieldwork and remote sensing identified active fault lines capable of generating earthquakes ranging from Mw 7.3 to 7.8, posing substantial threats to urban infrastructure [6]. Post-earthquake damage assessment research by Hosseini Varzandeh et al. (2024) following the Mw 7.3 Kermanshah earthquake revealed critical structural vulnerabilities that highlight deficiencies in current seismic design practices [7].

Urban planning considerations were addressed by Ahmadi and Kajita (2017) through their evaluation of seismic hazards' impact on Kabul's land development patterns [8]. Innovative assessment techniques were demonstrated by Alina et al. (2019) in Russia, where numerical simulations using the grid-characteristic method improved seismic stability evaluations for high-rise structures [9]. Region-specific code development was advanced by Keshavarz and Morteza (2017) in Bushehr, Iran, through their PSHA-derived uniform hazard spectrum [10], while Bambang et al. (2019) enhanced Tasikmalaya, Indonesia's hazard assessments by incorporating local fault systems and megathrust zone data [11].

Detailed zoning maps emerged from Alizadeh and Pourzeynali (2018) PSHA study of Amol, Iran, providing crucial data for infrastructure planning [12], paralleled by Ghodrati Amiri et al. (2015) development of seismic hazard maps and uniform hazard spectra for Kerman province [13]. Methodological comparisons were offered by Fahimi Farzam et al. (2018) through their examination of PSHA and DSHA applications in Iran [14], while Zare et al. (2022) focused specifically on Khark Island's acceleration zoning [15]. Dastjerdi et al. (2018) contributed to Bushehr's seismic understanding through combined deterministic-probabilistic fault analyses [16], and the NEA (2019) extended deterministic and probabilistic methodologies globally for nuclear facility safety assessments [17]. The Philippines' seismic modeling was advanced by Penarubia et al. (2020) through integrated fault movement and ground motion parameter analyses [18].

ShamsAldane et al. (2018) employed advanced probabilistic methods to assess risks along major Iranian faults, informing national hazard mapping efforts [19]. Bakhshi and Rezaie (2021) research on Sabzevar revealed important acceleration patterns, noting vertical accelerations at 50-60% of horizontal values and soil amplification effects consistent with Iran's Standard 2800 [20]. Oliver S. Boyd et al. (2007) provided critical probabilistic ground motion estimates for Afghan cities, identifying substantial earthquake risks of exceeding a peak ground acceleration (PGA) of 0.50g in Kabul, 35%g in Mazar-e Sharif, 28%g in Herat, and 13%g in Kandahar, establishing essential baseline data for regional seismic preparedness [1]. Collectively, these studies demonstrate significant progress in seismic hazard assessment techniques while highlighting the need for region-specific adaptations to address local geological conditions and infrastructure vulnerabilities.

Ezzodin et al. (2022) investigated the nonlinear seismic behavior of steel moment-resisting frames (MRFs) subjected to near-fault fling-step pulse-type ground motions. Using a random vibration-based model, they decomposed ground motions into pulse and non-pulse components and analyzed three MRFs (3-, 9-, and

20-story) via nonlinear time-history analysis in OpenSees. Their results showed that fling-step pulses increase seismic demands by ~50% in story drift and ~30% in roof displacement compared to non-pulse records, with taller structures experiencing greater deformations due to pulse effects [21].

Sharafi et al. (2025) developed a novel seismic vulnerability assessment framework for low-rise RC buildings in Afghanistan, addressing critical gaps in regional building codes. The study analyzed a comprehensive database of structures (2001–2022) from Afghan ministries, incorporating local seismic data and building attributes (materials, stories, construction year) to refine a modified Japanese Is Index. Using Capacity Spectrum Method (CSM) and STERA 3D dynamic analysis, the team created the Afghanistan Seismic Index (ASI), validated against existing methods. Results demonstrated ASI's effectiveness in region-specific evaluations, offering a tool to enhance structural safety, policy, and urban resilience in seismic zones [22].

A summary of these studies, presented in Table 1, highlights the significant contributions of various methodologies—ranging from deterministic and probabilistic analyses to field investigations and numerical simulations—in advancing regional seismic hazard assessment and preparedness.

Therefore, as indicated in Table 1, The present study offers an innovative approach by combining deterministic and probabilistic seismic hazard analysis for Kunduz Airport, a critical infrastructure in northern Afghanistan. This is among the first attempts to integrate advanced methodologies such as NGA-West2 ground motion prediction models and logic tree analysis to manage epistemic uncertainties for this region. Moreover, the study develops site-specific adjustment factors based on local soil properties (Vs30 values) and basin effects, which are rarely considered in previous Afghan seismic hazard assessments. A comparative evaluation of international seismic design codes, including Iranian Standard 2800, ASCE 7-16, and Eurocode 8, further enriches the outcomes and provides a scientific basis for safer and optimized earthquake-resistant designs.

The significance of this research lies in addressing a crucial national need. Kunduz Airport serves as a vital transportation hub and plays a key role during natural disasters and emergencies. Given the high seismicity of the Kunduz region, influenced by active fault systems like the Takhar and Kunduz faults, a precise understanding of seismic risk is essential. The absence of a national seismic code in Afghanistan increases the importance of conducting detailed hazard studies to support future development and disaster resilience initiatives. The findings of this research can also serve as a foundation for the seismic design of other critical facilities, including hospitals and emergency shelters, throughout northern Afghanistan.

This topic was chosen due to the current lack of advanced, location-specific seismic hazard studies for critical infrastructure in Afghanistan. Protecting strategic assets like airports is essential for national security and disaster management. Additionally, the tectonic setting of Kunduz, as part of the broader Alpine-Himalayan seismic belt, demands the application of state-of-the-art international practices in hazard assessment. Finally, the study aims to provide engineers, planners, and policymakers with scientifically grounded recommendations to improve the resilience and safety of future constructions.

2. Investigation method

This research employs a dual-method framework combining deterministic (DSHA) and probabilistic (PSHA) seismic hazard analyses to comprehensively evaluate earthquake risks at Kunduz Airport. The methodology addresses the unique challenges posed by Afghanistan's position in the seismically active Alpine-Himalayan belt while accounting for regional data limitations. The systematic workflow, illustrated in Figure 3, ensures robust hazard assessment through multiple verification stages.

The DSHA component of this study focused on evaluating worst-case seismic scenarios through a three-step methodology. First, active faults within a 200 km radius of the study area, including the Central

Badakhshan and Takhar faults, were identified through a synthesis of geological surveys and historical seismic data. Second, controlling earthquake magnitudes were estimated using multiple empirical relationships, specifically the Nowroozi (1985) equation for rupture length [23], the Ambraseys-Melville

Table 1. Summary of recent seismic hazard assessment studies.

Study	Year	Region	Methodology	Key Findings
Oliver S. Boyd et al. [1]	2007	U.S	Probabilistic Ground Motions	Several sources of seismicity are present in Afghanistan and contribute to appreciable seismic hazard for several major cities including Kabul, Mazar-e Sharif, Herat, and Kandahar.
Yucemen [4]	2013	Turkey	Probabilistic Analysis of Insurance Rates	Integration of seismic risks in insurance calculations.
Ghodrati Amiri et al. [13]	2015	Kerman - Iran	Seismic Hazard Analysis and Uniform Hazard Spectra	Developed seismic hazard maps and spectra for different regions of Kerman.
Ahmadi and Kajita [8]	2017	Kabul - Afghanistan	Urban Land Development and Seismic Evaluation	Evaluation of seismic impact on urban land development in Kabul.
Keshavarz and Morteza [10]	2017	Bushehr - Iran	Probabilistic Seismic Hazard Analysis	Determined uniform hazard spectrum for Bushehr Province.
Alizadeh and Pourzeynali [12]	2018	Amol - Iran	Probabilistic Seismic Hazard Analysis	Seismic hazard analysis with updated magnitude correlations; zoned peak ground acceleration for Amol.
Fahimi Farzam et al. [14]	2018	Iran	PSHA and DSHA	Overview of PSHA and DSHA methodologies; highlighted applications in seismic risk assessment.
Dastjerdi et al. [16]	2018	Bushehr - Iran	Deterministic and Probabilistic Methods	Analyzed seismic hazards for Bushehr, focusing on high-risk faults in the region.
ShamsAldane et al. [19]	2018	Iran	Probabilistic Seismic Hazard Analysis	Determined seismic risks and accelerations for major faults in Iran using advanced probabilistic methods.
Alina et al. [9]	2019	Russia	Grid-Characteristic Method	Assessed seismic stability of high-rise buildings using numerical simulations.
Bambang et al. [11]	2019	Tasikmalay - Indonesia	Probabilistic Seismic Hazard Analysis	Re-evaluated seismic hazards considering local fault systems and megathrust zones.
NEA [17]	2019	Global	Comparative PSHA	Analyzed probabilistic seismic hazards for nuclear power plants in areas with varying seismic activities.
Penarubia et al. [18]	2020	Philippines	Probabilistic Seismic Analysis	Developed a seismic hazard model for the Philippines, integrating fault movements and ground motion parameters.
Bakhshi and Rezaie [20]	2021	Iran	Deterministic and Probabilistic Methods	Southern and southwestern Sabzevar have higher peak acceleration due to proximity to faults.
Zare et al. [15]	2022	Khark Island - Iran	Probabilistic Seismic Hazard Analysis	Developed acceleration zoning maps for Khark Island, highlighting seismic risk in the Persian Gulf.
Ezzodin et al [21]	2022	Global	Nonlinear Time-History Analysis Under Simulated Fling-Step	A random vibration-based simulation model for nonlinear seismic assessment of steel structures in near-fault seismic zones in OpenSees**.**
Shnizai et al. [6]	2023	Kabul Basin -Afghanistan	Fieldwork and Remote Sensing	Identified active fault lines and estimated magnitude potential of Mw 7.3–7.8.
Bai et al. [5]	2024	Luding-China	Site Investigation	Observations on seismic isolation effectiveness.
Hosseini Varzandeh et al. [7]	2024	Kermanshah-Iran	Post-Earthquake Damage Assessment	Identified structural vulnerabilities in buildings after a Mw 7.3 earthquake.
Bakhshi et al. [3]	2025	Kunduz-Afghanistan	Deterministic and Probabilistic Methods, Seisrisk Software	Base acceleration: 0.411 g; need for updated building codes.
Sharafi et al [22]	2025	Afghanistan	Capacity Spectrum Method and STERA 3D Dynamic Analysis	Development and Validation of a Seismic Index for Assessing the Vulnerability of Low-Rise RC Buildings.

relationship for kilometer-scale measurements [24], and the Wells-Cooper Smith equations tailored to specific fault types [25]. Third, ground motions were predicted utilizing regionally-adapted attenuation models. These models were selected to account for local soil conditions, characterized by a Vs30 range of 250-300 m/s, the prevalence of thrust fault mechanisms, and local basin effects.

The PSHA methodology employed in this study integrated a comprehensive uncertainty analysis across several key components. Seismic sources were characterized through a combination of areal sources, incorporating spatially smoothed seismicity, along with specific fault sources and subduction interfaces pertinent to the Hindu Kush seismicity. Magnitude-frequency relationships for these sources were established using the Gutenberg-Richter law, with a b-value constrained to 1.0 ± 0.1 [26]. Ground Motion Prediction Equations (GMPEs) were incorporated through a weighted logic tree framework to account for epistemic uncertainties. This framework assigned weights to selected models: 40% to NGA-West2 models [27] (specifically for thrust mechanisms), 30% to regionally-adjusted models, and 30% to European analogs. The analysis subsequently computed hazard curves for four distinct return periods (72, 225, 475, and 2475 years) to encompass a range of design requirements [28].

The selection of SeisRisk III software was based on three key capabilities. First, its advanced computational functions enable simultaneous processing of multiple seismic sources and complex attenuation relationships while generating acceleration spectra. Second, the software's robust uncertainty quantification handles both epistemic uncertainties through logic trees and aleatory variability in ground motions. Third, its regional adaptability accommodates incomplete seismic catalogs, sparse fault data, and allows site-specific adjustments - crucial for Afghanistan's data environment [29].

The study incorporated multiple seismic standards to ensure comprehensive analysis. Iranian Standard 2800 [30] served as the primary reference due to its compatibility with the regional tectonic environment and thrust mechanisms. ASCE 7-16 [31] provided detailed response spectra and international benchmarking, while Eurocode 8 [32] contributed conservative near-fault analysis methods. The NGA-West2 models [27] were selected for their thrust mechanism compatibility and comprehensive spectral coverage. This multi-standard approach enabled cross-verification and development of site-specific recommendations.

The comprehensive data framework employed in this study integrated multiple sources to ensure maximum reliability for seismic hazard assessment. Fault data were primarily sourced from the USGS Quaternary Fault Database [33]. This was combined with a robust composite earthquake catalog, which merged historical seismicity records from the ISC Reviewed Event Bulletin (1964-2024) [34] and the USGS ANSS data (1900-present) [35]. Furthermore, site-specific Vs30 measurements obtained from 12 boreholes provided crucial information on local soil conditions [36]. The validation process of our results involved a rigorous comparison against available regional strong-motion records and historical intensity data, thereby ensuring consistency with observed seismic activity in the region.

The integrated DSHA-PSHA approach was selected because DSHA provides essential engineering parameters for worst-case scenarios while PSHA delivers comprehensive risk assessment considering all potential sources - particularly important for critical infrastructure [28]. SeisRisk III was chosen for its proven performance in data-scarce regions and ability to handle basin effects [29]. The multi-standard framework balances international best practices with regional adaptability, creating a solid foundation for developing Afghanistan's national seismic provisions.

This methodology establishes a robust, verifiable framework for seismic hazard assessment in data-limited regions. By combining advanced analytical techniques with practical engineering applications through the illustrated workflow (Figure 3), the approach delivers reliable results for airport design while setting a precedent for future seismic evaluations in Afghanistan. The integrated use of international standards with local adaptations provides both immediate design solutions and long-term guidance for national code development.

In light of this, the following procedures will describe the implementation phases of the research:

2.1. Equations for experiments to find the controlling earthquake

The controlling earthquake is a key concept in seismic hazard analysis, representing the earthquake scenario that is most likely to cause significant ground motion at the site of interest. The magnitude of the controlling earthquake is determined by analyzing the rupture length of nearby faults and their tectonic behavior. It is important to note that not the entire length of a fault is involved in energy storage and release during an earthquake; only the rupture length is considered in the calculation. The rupture percentage of faults varies depending on their size, typically ranging from 30% to 100% of the total fault length, with smaller faults often assumed to rupture entirely (100%).

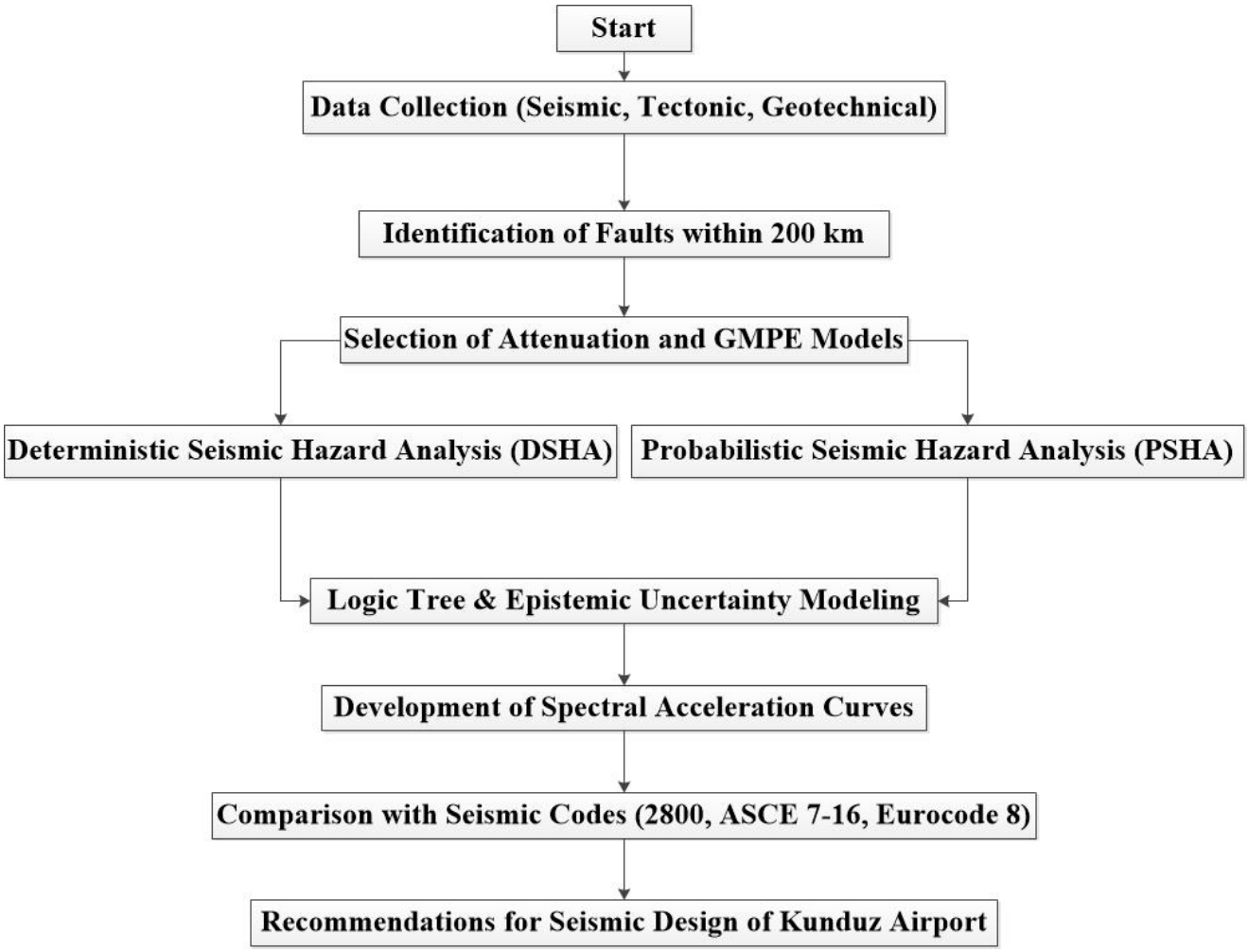

Fig. 3. Flowchart of Investigation Method.

To estimate the magnitude of the controller earthquake, several empirical relationships are employed. One of the most widely used is the Nowrooz experimental relation (Equation 1), which provides a reliable estimate of earthquake magnitude based on fault rupture length. This relationship is particularly useful for seismic hazard estimation and is often incorporated into logical tree calculations to account for uncertainties in fault behavior.

$$M_s = 1.25 + 1.244 \log L\,;\ L(m) \tag{1}$$

The proposed Ambraseys-Melville models (Equation 2) [37] as well as the four Wells-CooperSmith equations (Equations 3 to 6) [10] can also be used to find the controller earthquake (Table 2).

$$M_s = 5.4 + \log L\,;L(km) \tag{2}$$

Table 2. Unified Summary of Empirical Magnitude–Rupture Length Relations [10,38].

Fault type	Magnitude span	Estimated equation	Equation number
Slip fault	5.8-6.1	$M_s = 5.16 + 1.12 \log L\,;(km)$	(3)
Reverse fault	5.7-4.4	$M_s = 5 + 1.12 \log L\,;(km)$	(4)
Normal fault	5.7-2.3	$M_s = 4.86 + 1.32 \log L\,;(km)$	(5)
All faults	5.8-2.1	$M_s = 5.08 + 1.16 \log L\,;(km)$	(6)
Slip fault	-	$M_s = 1.404 + 1.16 \log L\,;(km)$	(7)
Reverse fault	-	$M_s = 2.021 + 1.142 \log L\,;(km)$	(8)
Normal fault	-	$M_s = 0.809 + 1.341 \log L\,;(km)$	(9)

The Zareh's proposed model is given in relation (10) [15].

$$M_s = 0.91 \ln L_R + 3.66 \quad (10)$$

In these relationships (Equations 1 to 10), M_S represents the surface magnitude of the earthquake, and L_R denotes the rupture length. The rupture length of the fault, L_R, is expressed in meters in the Nowroozi relation and in kilometers in the other equations. According to Nowroozi, the rupture length is equivalent to 50% of the total fault length (L_F), i.e., $L_R = 0.5\ L_F$. However, Zareh considers L_R to be 37% of the fault length, i.e., $L_R = 0.37\ L_F$ [15].

The selection of ground motion prediction equations (GMPEs) for this study was carefully conducted through a systematic evaluation process considering multiple technical criteria essential for reliable seismic hazard assessment in the Kunduz region (Table 3).

Table 3. GEMPES weight.

Category	GMPE Name	Weight
NGA-West2	Campbell and Bozorgnia (2014)	20%
NGA-West2	Boore et al. (2014)	20%
European Model	Akkar and Bommer (2010)	30%
Regional Analog	Zare et al. (2007) [15]	30%

The primary basis for selection included tectonic compatibility with Afghanistan's active continental collision environment, appropriate magnitude-distance coverage (Mw 5.0-7.5, R=0-100 km), and explicit treatment of site-specific conditions (NEHRP Site Class D, Vs30=250-300 m/s). Global NGA-West2 models (Campbell and Bozorgnia 2014, Bozorgnia et al. 2014) were prioritized due to their robust treatment of thrust mechanisms and hanging wall effects relevant to nearby reverse faults, while Zhao et al. (2016) was included in the seismic hazard assessment due to its specific calibration for the complex tectonic settings and seismicity characteristic of the Asian collision zone, ensuring more accurate ground motion predictions in this region [39]. Regionally-developed equations (Nowroozi 2005, Mahdavian 2006) supplemented the analysis to account for local crustal properties and attenuation characteristics. This multi-model approach enabled comprehensive uncertainty quantification through logic tree weighting, with particular attention to near-field directivity effects from the Darafshan and Central Badakhshan faults. The selected GMPEs collectively provide complete spectral coverage (PGA to 5s) necessary for diverse airport structures, from stiff fuel storage facilities to flexible control towers. Vertical motion predictions were specifically considered for runway and critical infrastructure design. All equations were cross-validated against available regional strong-motion data where possible, and adjusted for basin depth effects influencing long-period ground motions. This methodology aligns with SSHAC guidelines for probabilistic seismic hazard analysis while addressing the unique challenges of Afghanistan's seismic environment through balanced incorporation of global best practices and regionally-calibrated relationships.

2.2. Calculating the supervisor earthquake for deterministic hazard assessment

Following the faults' classification based on mechanism and the use of the Nowrooz, Ambersis-Melville experimental relations to calculate the rupture length—which in this study is 0.37 for faults over 100 km and 0.5 times for faults under 100 km. The Solmaz model and Wells-Coopersmith were utilized to calculate the controlling earthquake's magnitude. The fault rupture area was used to calculate the magnitude, and Table 4 shows the results for each defect.

Ramazi- Schenk model is in the general form of Equation (11) and the proposed coefficients of this equation are expressed in Table (5) [12].

$$a = a_1(a_2 + d + H)^{a_5} exp(a_6 M_s); \quad H = |d - a_3|^{a_4} \qquad ; a \quad = {}^{cm}/_{s^2} \tag{11}$$

Table 4. Earthquake controller for faults located less than 200 kilometers from Kunduz city.

Row	Fault name	Method	Fault length	Rupture length	Estimated magnitude by exprimental equations				M_s=M_w
					Nowroozi	Ambraseys	Wells	Solmaz	
			Km	Km	0.25	0.25	0.25	0.25	
F_1	Darafshan	Normal	215.851	79.87	7.36	7.30	7.07	7.38	7.28
F_2	Central Badakhshan	Normal	203.833	75.425	7.33	7.28	7.04	7.35	7.25
F_4	Hari rod	Normal	17.257	17.257	6.53	6.64	6.29	6.49	6.49
F_5	Chaman	Normal	64.9	32.45	6.87	6.91	6.61	6.86	6.81

Table 5. Proposed Ramazi-Schenk connection coefficients [12].

Acceleration component		a_1	a_2	a_3	a_4	a_5	a_6
a_h	Soil	4000	20	16	0.63	-2.02	0.8
	Rock	4000	20	16	0.63	-2.11	0.79
a_v	Soil	4000	20	16	0.48	-1.75	0.53
	Rock	4000	20	16	0.48	-1.75	0.53

Campbell- Bozorgnia attenuation equation used in this relationship is generally Equation (12) and the coefficients of this model are shown by Table (6) [13].

$$ln\,Y = c_1 + c_2 M_w + c_3(8.5 - Mw)^2 + c_4\, ln(\{R_s{}^2 + [(c_5 + c_6\{S_{PS} + S_{SR}\} + c_7 S_{HR}) exp(c_8 M_w + c_9\{8.5 - M_w\}^2)]^2\}^{1/2}) + c_{10} F_{SS} + c_{11} F_{RV} + c_{12} F_{TH} + c_{13} S_{HS} + c_{14} S_{PS} + c_{15} S_{SR} + c_{16} S_{HR}; Y = g \tag{12}$$

Table 6. Bozorgnia attenuation equations 2000: Suggested constants and coefficients [13].

Uncorrected horizontal component of acceleration	C1=-2.896	C2=0.812	C3=0	C4=-1.318	C5=0.187	C6=-0.029
	C7=-0.064	C8=0.616	C9=0	C10=0	C11=0.179	C12=0.307
	C13=0	C14=-0.062	C15=-0.195	C17=-0.320	σ =0.509	
Uncorrected vertical component of acceleration	C1=-2.807	C2=0.756	C3=0	C4=-1.391	C5=0.191	C6=0.044
	C7=-0.014	C8=0.544	C9=0	C10=0	C11=0.091	C12=0.223
	C13=0	C14=-0.096	C15=-0.212	C17=-0.199	σ =0.548	

The classification of soil type in the Campbell-magnitude reduction relationship is as shown in Table (7):

Table 7. Division soil types in Bozorgnia attenuation equation. [13].

Holocene Soil (HS)	V_{S30}=290m/s	S_{HS}=1	S_{PS}=0	S_{SR}=0	S_{HR}=0
Pleistocene Soil (PS)	V_{S30}=370m/s	S_{HS} =0	S_{PS} =0	S_{SR} =1	S_{HR}=0
Soft Rock (SR)	V_{S30}=420m/s	S_{HS} =0	S_{PS} =0	S_{SR} =1	S_{HR}=0
Hard Rock (HR)	V_{S30}=800m/s	S_{HS} =0	S_{PS} =0	S_{SR} =0	S_{HR}=1

The classification of the fault mechanism in the Campbell-magnitude reduction relationship is as described in Table (8):

Table 8. Division faulting mechanism [13].

Strike Slip	F_{TH}=0	F_{SS}=1	F_{RV}=0
Reverse	F_{TH}=0	F_{SS}=0	F_{RV}=1
Thrust	F_{TH}=1	F_{SS}=0	F_{RV}=0

In Khademi attenuation equation, the model can be used in the general form of relation (13) and the table of its proposed coefficients is shown by Table (9) [20].

$$Y = C_1\, exp(C_2 M_W)((R + C_3\, exp(C_4 M_W))^{C_5}) + C_6 S;\ Y = g \quad (13)$$

Table 9. The suggested coefficients for the Khademi attenuation equations in 2002 [20].

acceleration component		C_1	C_2	C_3	C_4	C_5	C_6	S
Horizontal component	Soil	0.040311	0.417342	0.001	0.65	-0.035852	-0.035852	1
	Rock	0.040311	0.417342	0.001	0.65	-0.035852	-0.035852	0
Horizontal component	Soil	0.0015	0.8548	0.001	0.4	-0.4	-0.463	1
	Rock	0.0015	0.8548	0.001	0.4	-0.4	-0.463	0

Nowroozi attenuation equation (2005) used in this section is given in Equation (14) and its proposed coefficients are shown in Table (10) [19].

$$ln(A) = c_1 + c_2(M_W - 6) + c_3\, ln\left(\sqrt{EPD^2 + h^2}\right) + c_4 S;\ A = cm/s^2 \quad (14)$$

Table 10. Suggested coefficients for Nowroozi attenuation equations (2005) [19].

Acceleration component		C_1	C_2	C_3	C_4	H	σ	S
Horizontal component	Gravel & sand	7.969	1.220	-1.131	0.212	10	0.825	1
	Rock & Alluvial	7.969	1.220	-1.131	0.212	10	0.825	0
Horizontal component	Gravel & sand	7.262	1.214	-1.094	0.103	10	0.773	1
	Rock &Alluvial	7.262	1.214	-1.094	0.103	10	0.773	0

In Mahdavian attenuation equation (2006) [13], the model used in Equation (15) is shown and its proposed coefficients are shown in Table (11) [13].

$$Log\ (y) = a + bM_S + c\ log(R) + dR;\ y = cm/s^2 \quad (15)$$

Table 11. Suggested coefficients for the Mahdavian attenuation equations 2006 [13].

	floor	Earthquake parameters	A	b	C	D	Σ
Alborz and Central Iran	of stone	PGAH	2.058	0.243	-1.02	-0.000875	0.219
		PGAV	1.864	0.232	-1.049	-0.000372	0.253
	of soil	PGAH	1.912	0.201	-0.79	-0.00253	0.204
		PGAV	1.76	0.232	-1.013	-0.000551	0.229

In Ghodrati attenuation equation (2007) [40], the model used is the general form of Equation (16) and its proposed coefficients are specified in Table (12) (Iman A, 2015) [40].

$$Lny = C_1 + C_2 M_S + C_3 L_n(R + C_4 exp[M_S]) + C_5 R;\ y = cm/s^2 \quad (16)$$

Table 12. Suggested constants coefficients for the Ghodrati attenuation equation 2007 [40].

	Floor	Earthquake parameters	C1	C2	C3	C4	C5	Σ
Alborz and Central Iran	stone	PGAH	4.15	0.623	-0.96	-	-	0.478
		PGAV	3.46	0.635	-0.996	-	-	0.49
	soil	PGAH	3.65	0.678	-0.95	-	-	0.496
		PGAV	3.03	0.732	-1.03	-	-	0.53

For definitions of parameters used in attenuation equations, refer to the Appendix.

The most common measure of amplitude in ground motion is the maximum horizontal acceleration (PGA_H). PG_{AH} for each motion component is the largest absolute value of horizontal acceleration recorded by that accelerometer component. Geometric mean or maximum of the two components. In engineering applications, it is often assumed that the maximum vertical acceleration (PGA_V) is two-thirds of the maximum horizontal acceleration (PGA_H). Weights for GMPE branches were determined based on tectonic applicability, region-specific calibration, and expert judgment, in accordance with the SSHAC Level 2 guidelines. Due to limited local strong-motion data, regional analogs and published models were used as proxies.

3. Data analysis

The data and values for the both horizontal and vertical accelerations acquired are used to examine and compare the earthquake risk analysis methods in this section. The SeisRisk III software of acceleration curves was utilized for this purpose in order to estimate the acceleration components using a probabilistic manner. The results of this process were then compared with the values produced for the acceleration component by a deterministic method.

3.1. Deterministic seismic hazard analysis

As outlined earlier, deterministic seismic risk assessment is used to assess structures like nuclear power stations, massive dams. These are oil resources, and other critical infrastructure where failure would have disastrous consequences. In this regard, using the experimental equation of Nowroozi, Ambersiz-Melville, Wells-Coopersmith, and Sulmaz to analyze the deterministic seismic hazard, after determining the faults of Kunduz city within a radius of 200 km and determining the process of the fault, the distance from the fault to the site, and also according to the greatest risk determined for each fault. The action took place using attenuation equations to determine the maximum components of both horizontal and vertical acceleration based on two types of soil: the first type of soil, encompassing types I and II, and the second type of soil, which includes kinds III and IV of the standard No. 2800. Lastly, the logic tree and weight coefficient of 0.4, 0.3, 0.4, and 0.41 were optimized for the highest acceleration derived from the Nowroozi, Ambersiz-Melville, Wells-Coopersmith, and Solmaz reduction relations, respectively (Figure 4). For those attenuation equations for which weight the coefficients were not proposed, the coefficients obtained from the formulas themselves and the weighting coefficients got for each of the attenuation equations were selected to obtain the maximum value for these attenuation equations. These weight coefficients, referred to as the optimal weight coefficients, were proposed for each of the decrease relations and were chosen in order to optimize. The calculations' outcomes are displayed in Table (13).

Table 13. Results of determinant risk analysis in Kunduz.

Row	Fault name	Closest distance	Estimated magnitude	Acceleration component			
				Soil types I and II		Soil type III and IV	
		Km	Ms=Mw	Horizontal	Vertical	Horizontal	Vertical
F_1	Darafshan	91.633	7.28	0.3	0.25	0.31	0.3
F_2	Centeral Badakhshan	167.925	7.25	0.15	0.37	0.4	0.3
F_4	Hari rod	183.451	6.49	0.19	0.31	0.37	0.3
F_5	Chaman	183.5	6.81	0.4	0.41	0.35	0.38

According to Table (13):

- In type 1 soil, the Chaman fault is associated with the maximum ground acceleration, which ranges from 0.4 to 0.41.
- In type II soil, the Central Badakhshan fault is associated with the maximum ground acceleration, which ranges from 0.4 to 0.3.

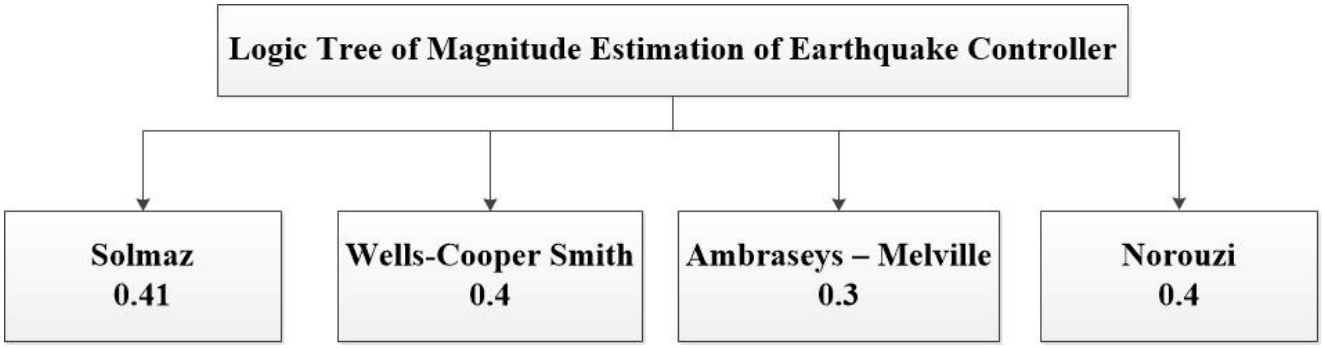

Fig. 4. Logic tree of magnitude estimation of controller earthquake.

The logic tree framework presented in Figure 4 systematically estimates the controlling earthquake magnitude through integration of multiple seismic parameters. The structure incorporates three primary components: (1) fault typology classification, (2) seismic source characterization, and (3) maximum credible earthquake (MCE) assessment. At each nodal point, alternative scientific interpretations are weighted to probabilistically quantify epistemic uncertainties. This multi-branch architecture provides a robust platform for synthesizing diverse geological and seismological datasets, significantly enhancing the reliability of magnitude estimates for both deterministic (DSHA) and probabilistic (PSHA) seismic hazard analyses. The methodology's strength lies in its explicit treatment of parameter uncertainty through discrete probability-weighted branches, where each path represents a scientifically valid interpretation of the available evidence.

3.2. Probabilistic seismic hazard analysis

Using SeisRisk III software and seismic springs, good seismic parameters, attenuation equations, and Khademi, Nowroozi, and Mahdavian relations—all of which have weight coefficients of 0.10, 0.14, 0.17, 0.19, 0.20, and 0.20, respectively—are used in this method to determine the maximum horizontal and vertical acceleration curves for the region. These curves are based on two types of soil: types I and II, and types III and IV of the standard No 2800, respectively (Figure 5 to Figure 8). It should be mentioned that Bender and Perkins SeisRisk III program for probabilistic risk analysis [14].

This software is able to optimize the parameters of ground movement in the area by taking into account the design levels, appropriate levels of danger, and all the probabilities and unpredictability in order to calculate

the magnitude of the region as well as the rate of earthquakes. This is done after defining seismic sources and determining diminution equation, using seismicity parameters such as those obtained from the Kijko method [41].

To perform fast and accurate hazard analysis Design parameters (base acceleration, spectral acceleration, plot spectrum) and parameters associated with seismic sources, seismicity, and reduction connection are calculated for each risk level via a probabilistic conjunction, and the evaluation is based on the T_R return period or the probability of an annual occurrence (Equation 17).

$$P = \frac{1}{T_R} \tag{17}$$

T_R (Return Period) represents The average time of occurrence of seismic activity within the target range of particular magnitude, while P (Annual Probability) is the reversal of the return period, corresponding to the annual seismic probability [42].

Equations (18), (19) can be used to calculate the the chance of an earthquake (q) happening during the structure's useful life (n years), that will yield the period of return or probability of an annual earthquake occurring, enabling a probabilistic assessment of seismic risk for Kunduz Province using SeisRisk III software.

$$T_R = \frac{1}{1-(1-q)^{1/n}} \tag{18}$$

$$P = 1 - (1-q)^{1/n} \tag{19}$$

In this study, according to the Seismic Different design levels with a return period of 72, 225, 475, and 2475 years have been looked at, according to Improvement Instruction of Existing Buildings (2002). These stages are:

1. Selective Hazard Levels 1: This risk level is calculated on a 72-year return time (a 50% chance of an event occurring in 50 years).
2. Selective Hazard Level 2: Based on a 20% probability of recurrence in 50 years, or a 225-year return period, this category of risk is determined.
3. Risk level 1: Given a 10% chance of an occurrence occurring in 50 years, or a 475-year return time frame, this risk level is established. The Iranian Standard 2800 Regulation refers to preparing earthquakes as hazard level 1 (DBE).
4. Risk Level 2: Based on a 2% possibility of an occurrence occurring in 50 years, or a 2475-year return time frame, this risk level is established. Standard 2800 refers to earthquake hazard level 2 as MPE.

3.2.1. Seismic acceleration response curves for different soil types

These figures provide site-specific seismic design input for performance-based evaluation of critical infrastructure such as airports, ensuring resilience under rare and extreme ground motion scenarios. And also figures 5 through 8 present seismic response curves that illustrate the spatial variation of ground acceleration components in both horizontal and vertical directions across different soil categories. These curves, derived from a probabilistic seismic hazard assessment with a 2% probability of exceedance in 50 years (return period of 2475 years), illustrate seismic demands essential for performance-based design of critical facilities such as airports, corresponding to a return period of approximately 2475 years. This level of seismic hazard is typically used for critical or essential facilities that must remain operational during major seismic events.

Figure 5 displays the horizontal acceleration response curves for soil types I and II.

- Soil Type I generally corresponds to hard rock or very stiff soil conditions with minimal amplification effects.

- Soil Type II consists of medium-dense to dense soils that allow moderate amplification of seismic waves.
- These curves provide insight into the expected horizontal shaking intensity that structures may experience depending on the underlying soil properties.

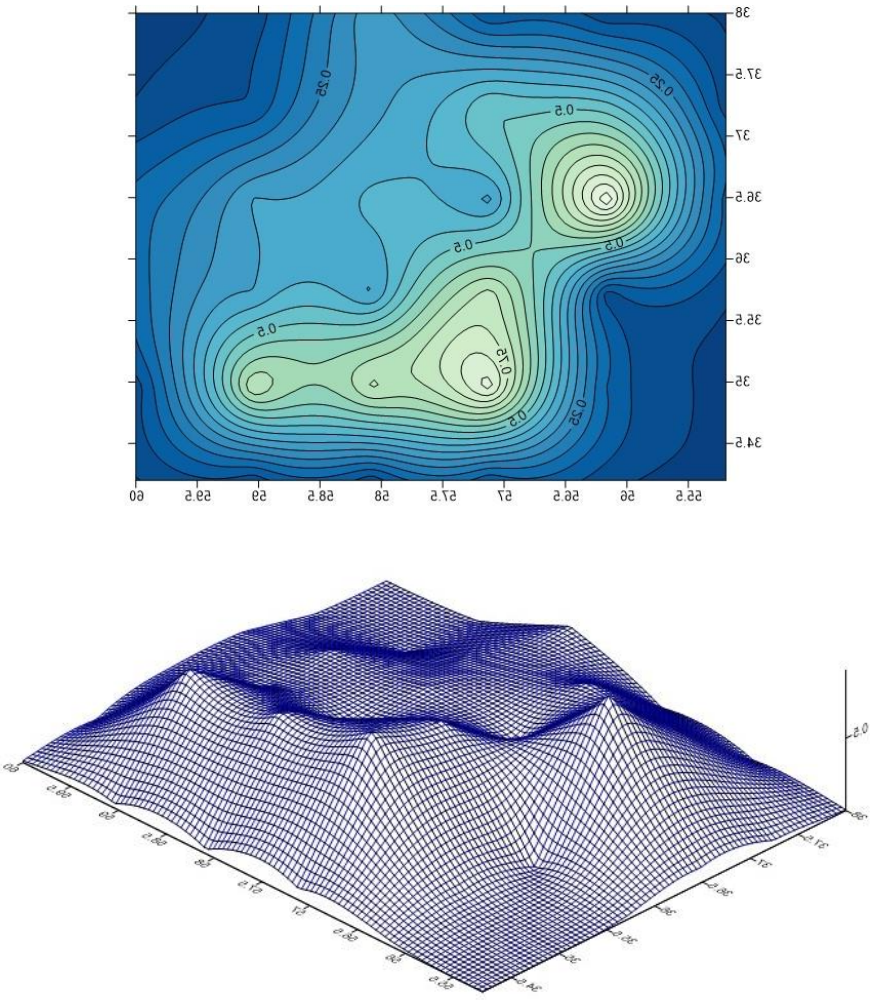

Fig. 5. The region's horizontal acceleration component Curves for soil types I and II, with a 2% the probability.

Figure 6 illustrates the vertical acceleration component for the same soil types. Although vertical ground motion is often lower in amplitude than horizontal motion, it can still impose significant dynamic effects on certain structural systems, especially those with long spans or irregular geometries.

Figure 7 shows horizontal acceleration curves for soil types III and IV, which represent progressively weaker and softer soil conditions.

- Soil Type III includes soft soils such as loose sand and silty clay, which are known to amplify seismic waves significantly.
- Soil Type IV refers to very soft or artificial fill soils, which may exhibit extreme amplification effects during seismic shaking.
- These conditions are associated with higher seismic demands on structures and require more conservative design approaches.

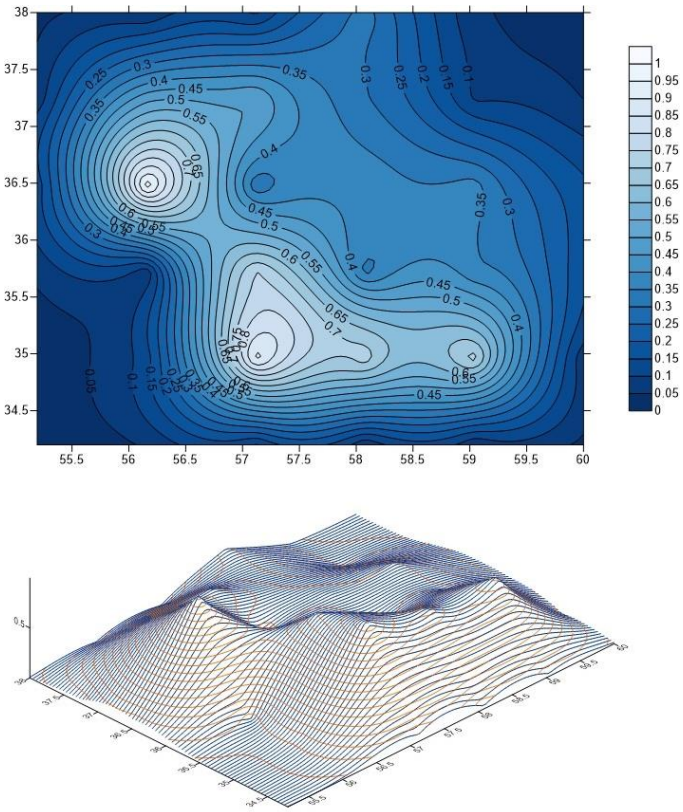

Fig. 6. The region's vertical acceleration component Curves for soil types I and II, with a 2% the probability.

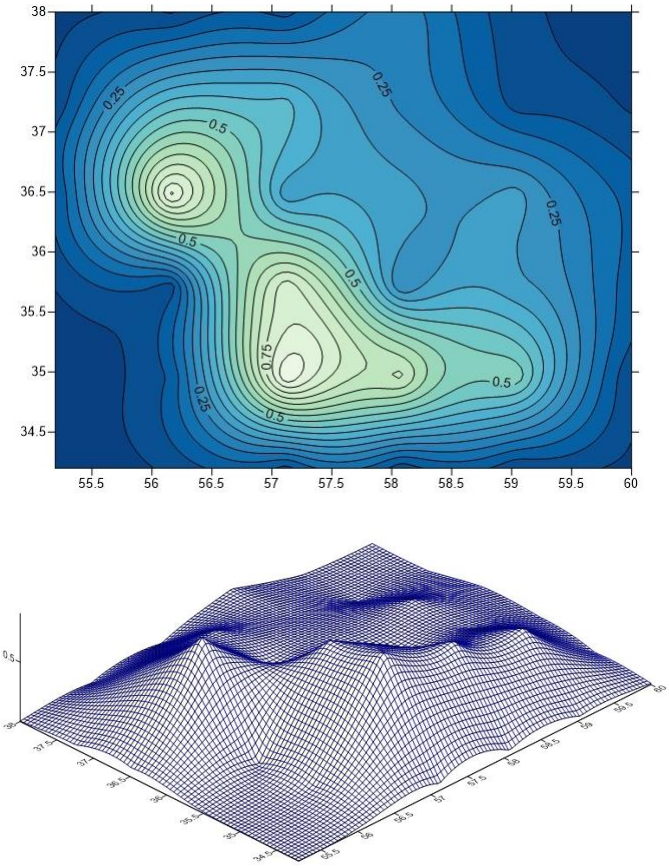

Fig. 7. The region's horizontal acceleration component Curves for soil types III and IV, with a 2% the probability.

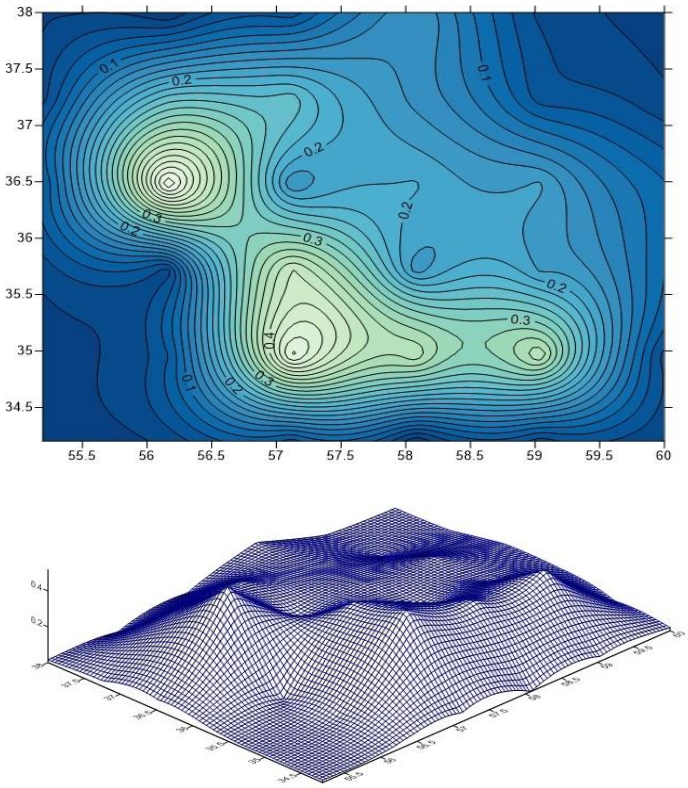

Fig. 8. The region's vertical acceleration component Curves for soil types III and IV, with a 2% the probability.

Finally, Figure 8 presents the vertical acceleration curves for soil types III and IV. These curves are crucial for understanding the potential vertical loading effects on structural elements, particularly in regions with soft soil profiles where vertical amplification may be non-negligible.

The presented curves (Figures 5 to 8) serve as a foundational component in the development of site-specific design spectra, allowing for the incorporation of local geotechnical conditions into seismic design practices. They are particularly useful in evaluating the performance of structures under rare but high-magnitude earthquake scenarios, aiding in the selection of appropriate structural systems and foundation designs.

3.3. Comparing probabilistic vs deterministic risk assessments

The maximum both vertical and horizontal acceleration parts in these two methods (deterministic and probabilistic) are based on the city of Kunduz, that longitude and latitude coordinates are 68.8 and 36.8, respectively (calculated by the deterministic method), with the data taken from the curves representing the maximum horizontal component. Additionally, Table 14 shows the results of comparing the vertical acceleration for danger level 2 with a 2% probability of an occurrence (referred to as the highest earthquake tolerance in the norm no. 2800 regulation).

Table 14. Comparison of the results of deterministic and probabilistic analysis for Kunduz airport.

Acceleration components								Type of analysis	Coordinates	
Probabilistic				Deterministic						
IV, III		II, I		IV, III		II, I		Type of soil		
Vertical	Horizontal	Vertical	Horizontal	Vertical	Horizontal	Vertical	Horizontal	Extension / Hazard level	Latitude	Longitude
0.54	0.5	0.411	0.392	0.3	0.4	0.41	0.4	2%	36.8	68.8

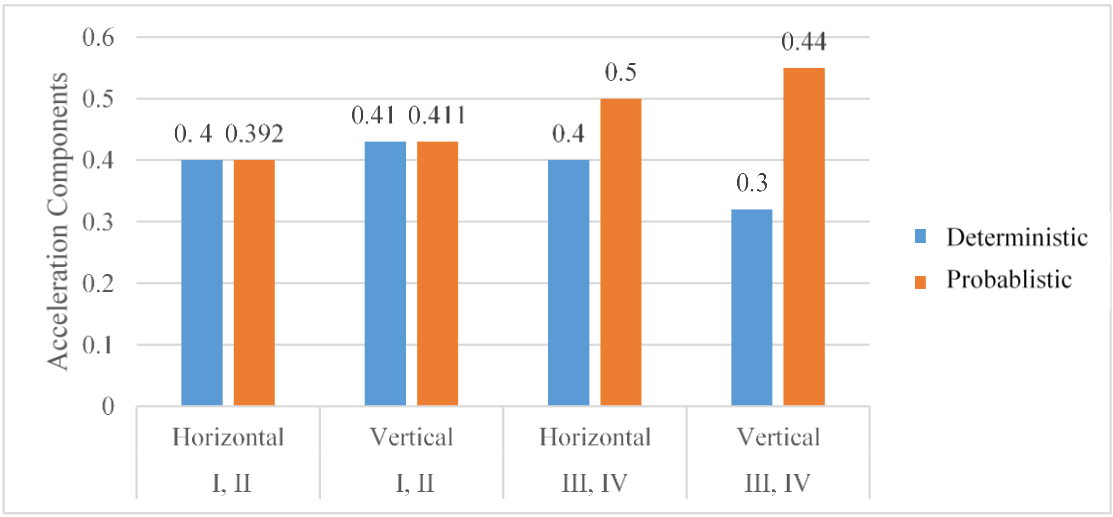

Fig. 9. Comparison of the results of deterministic and probabilistic analysis for Kunduz airport.

Based on Table 14 and Figure 9, PSHA generally produces higher ground acceleration values (e.g., 0.5g horizontal for Soil Type IV-III) than DSHA (0.4g) due to its more comprehensive approach to risk assessment. PSHA considers the cumulative effect of all potential earthquakes from various sources, weighting them by their probability of occurrence, rather than focusing on a single "worst-case" event like DSHA.

Furthermore, PSHA explicitly incorporates both aleatory uncertainty (natural randomness in ground motion) and epistemic uncertainty (lack of knowledge). It accounts for the full range of possible ground motions using statistical distributions and uses logic trees to model uncertainties in seismic parameters, especially crucial in data-scarce regions. This thorough, probabilistic treatment of all seismic scenarios and their associated uncertainties naturally leads to more conservative and typically higher hazard estimates, providing a more robust basis for seismic design.

3.4. Comparing the results of the methodologies (deterministic vs probabilistic) with the region's data that is currently accessible

Comparing the results of deterministic and probabilistic methods based on the data that is currently available in the region, assuming the magnitude of Mw, and centered on the city of Kunduz, as indicated in Table (15).

Table 15. Comparison of the results extracted from the methods (determinative and probabilistic) with the available data of the region.

Coordinate		Available data of the region		Results	
longtitude	Latitude	Historically	With instrument	Probabilistic	Deterministic
68.8	36.8	7.5	7.7	7.35	7.28

The values of the data in the region show greater significance, but and align closely with the computational result the computational values, as shown in Table (15). This indicates that the regional data offers a reliable and robust representation of seismic activity in the area. While the computational values are based on theoretical models, their close alignment with the regional data highlights the accuracy and relevance of both datasets. Therefore, although the regional data holds notable significance, the consistency between the two sets of values strengthens confidence in utilizing either for further analysis and decision-making in seismic hazard assessments.

The data and values for both horizontal and vertical accelerations are used to examine and compare earthquake risk analysis methods in this section. EZ-FRISK software was utilized to estimate the acceleration components using a probabilistic approach. The results were then compared with the values produced for the acceleration components by a deterministic method.

4. Conclusions and future work

This study conducted a detailed seismic hazard assessment of Kunduz Airport, which is strategically located in the active Alpine-Himalayan belt in northeastern Afghanistan. To comprehensively assess the seismic hazards, we used both probabilistic (PSHA) and deterministic (DSHA) methods. Our analysis carefully incorporated site-specific soil conditions (Vs30 values ranging from 250 to 300 m/s), accurate historical seismic data, and extensive regional tectonic information. Key findings from this study are as follows:

- The PSHA method, known for its comprehensiveness and ability to account for inherent uncertainties, yielded an average peak ground acceleration (PGA) of 0.411g for the 2475-year return period. This result emphasizes the importance of probabilistic approaches, especially when designing critical infrastructure such as airport facilities.
- In the deterministic analysis, the Chaman fault emerged as the main controlling seismic source, dictating a maximum PGA of 0.41g under type I soil conditions. While DSHA provides valuable insights into boundary scenarios, our comparison demonstrated its tendency to underestimate the true hazard compared to the more comprehensive PSHA framework. This emphasizes the essential nature of probabilistic assessments in hazard assessment.
- The calculated hazard levels consistently confirmed the high seismic hazard of the region. Furthermore, the strong alignment of our findings with instrumental records and historical regional earthquake data confirmed the validity and accuracy of our adopted methodology.
- A comparative analysis of international design codes (including Iran Standard 2800, ASCE 7-16, and Eurocode 8) revealed significant differences, especially regarding base shear and spectral acceleration values. This divergence strongly emphasizes the urgent need to adjust and update seismic codes in Afghanistan to reflect the specific tectonic and geotechnical conditions of the country.

This study establishes a fundamental framework for seismic hazard reduction not only for Kunduz but also for other vulnerable areas across Afghanistan. By integrating insights from PSHA and DSHA results with detailed geotechnical data and comparisons to international standards, this research provides valuable information for developing resilient infrastructure programs.

The results of this study also point to critical weaknesses and opportunities and indicate that the following important areas should be the focus of future research and national policymaking:

- Revise National Seismic Design Standards: It is essential to update Afghanistan’s current seismic design codes. This update should include recent local geological and geotechnical data, including basin effects analysis and soil strengthening factors based on the more accurate Vs30.
- Improving ground motion characterization: Future efforts should focus on improving ground motion characterization and refining hazard estimation through detailed microzonation studies and advanced time history dynamic nonlinear analyses.
- Calibration of damping relationships: To further reduce epistemic uncertainty and increase the reliability of hazard assessment, it is essential to improve the calibration of ground motion prediction equations (GMPEs) using local strong motion records.

Collectively, these proactive initiatives will play a pivotal role in developing performance-based and context-sensitive design guidelines, ultimately enhancing Afghanistan's seismic resilience across all critical infrastructure sectors.

Funding

This research did not receive any specific grant from funding agencies in the public, commercial, or not-for-profit sectors.

Conflicts of interest

The authors declare that they have no known competing financial interests or personal relationships that could have appeared to influence the work reported in this paper.

Authors contribution statement

Mohammad Jawad Rahimi: Formal analysis, Data curation, Project administration, Resources, Validation, Visualization, Roles/Writing –original draft, Writing –review & editing.

Abdulhai Kaiwaan: Formal analysis, Methodology, Visualization.

Shamsullah Anwari: Data curation, Formal analysis, Methodology, Supervision, Visualization.

Sayed Javid Azimi: Resources, Supervision, Roles/Writing –original draft, Writing –review & editing.

Zaher Rezaie: Conceptualization, Formal analysis, Investigation, Project administration, Resources, Supervision, Validation, Visualization, Roles/Writing –original draft, Writing –review & editing.

Appendix. comparative tables and supplementary analysis

This appendix provides supporting materials and additional analyses that complement the findings presented in the main manuscript. The included tables and figures offer further details on seismic hazard parameters, empirical relationships, and comparative evaluations referenced throughout the study.

Table A.1. Comparative rupture lengths from empirical relations.

Magnitude (Mw)	Nowroozi (km)	Wells-Coppersmith (km)	Solmaz (km)	Zareh (km)
6.0	15	17	16	13
6.5	25	28	27	23
7.0	40	42	41	36
7.5	65	68	66	58

Table A.2. GMPE logic-tree branches and weighting rationale.

GMPE Model	Mechanism Type	Justification	Weight (%)
NGA-West2 (2014) [27]	Thrust	Best for thrust faults near site, US-based validation	40
Zhao et al. (2016) [39]	Thrust	Calibrated for Asian collision zones	30
Nowroozi (2005) [19]	Reverse	Locally developed for Iran/Afghanistan region	30

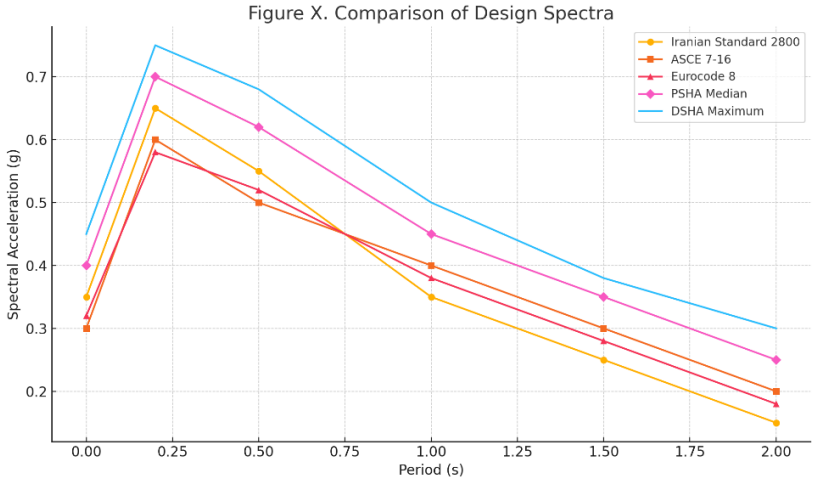

Fig A.1. Comparative plot of code-based spectra (2800, ASCE 7-16, Eurocode 8), PSHA, and DSHA (to be inserted).

[This plot should show the response spectra on the same axes for clarity. Each curve should be labeled, and the PGA values should be identified.]

The parameters related to equations (11) to (16) are as follows:

- y: horizontal component of maximum ground acceleration in unit g (cm/s^2)
- d: Distance to the fault surface (on the ground)
- h: Focal depth
- R: Focal distance
- R_S or R_{seis}: the closest distance of the earthquake rupture surface
- M_S: Magnitude of earthquake surface waves
- M_W: instantaneous magnitude
- EPD: Engineering seismic demand parameter or desired response of structure
- S_{SR}: soft rock site factor (1 for soft rock and 0 for other conditions)
- S_{HR}: hard rock location factor (1 for hard rock and 0 for other conditions)
- F: fault mode factor (zero for strike-slip and one for other modes)
- V_{S30}: Shear wave speed at a depth of 30 meters in table (6).
- PGA_H and PGA_V: Maximum horizontal acceleration and maximum vertical acceleration in table (12).

References

[1] Boyd OS, Mueller CS, Rukstales KS. Preliminary earthquake hazard map of Afghanistan. US Geol Surv Open-File Rep 2007:1137.

[2] Ruleman CA, Crone AJ, Machette MN, Haller KM, Rukstales KS. Probable and Possible Quaternary Faults of Afghanistan. US Geol Surv Open-File Rep 2007;1103.

[3] Bakhshi H, Rahimi MJ, Rastin MN, Rezaie Z. Seismic Hazard Evaluation and Accelerated Curves for Kunduz City (Afghanistan). Comput Eng Phys Model 2025;8:1–24. https://doi.org/10.22115/cepm.2024.490533.1349.

[4] Yucemen MS. Probabilistic assessment of earthquake insurance rates for Turkey. Nat Hazards 2005;35:291–313. https://doi.org/https://doi.org/10.1007/s11069-004-6485-8.

[5] Bai W, Dai J, Liu R, Shao Z, Yang Y, Jiang T, et al. Site investigation on seismic performance of 7 isolated buildings during the 2022 Luding Ms 6.8 earthquake. J Build Eng 2024;89:109224. https://doi.org/10.1016/j.jseaes.2023.105925.

[6] Shnizai Z, Walker R, Tsutsumi H. The Chaman and Paghman active faults, west of Kabul, Afghanistan: Active tectonics, geomorphology, and evidence for rupture in the destructive 1505 earthquake. J Asian Earth Sci 2024;259. https://doi.org/10.1016/j.jseaes.2023.105925.

[7] Varzandeh SSH, Mahsuli M, Kashani H, Dolatshahi KM, Hamidia M. Seismic performance of buildings during the magnitude 7.3 Kermanshah, Iran earthquake. J Build Eng 2024;91:109522. https://doi.org/10.1016/j.jobe.2024.109522.

[8] Ahmadi AS, Kajita Y. Evaluation of urban land development direction in Kabul city, Afghanistan. Conf. ID, 2023, p. 79.

[9] Breus A, Favorskaya A, Golubev V, Kozhemyachenko A, Petrov I. Investigation of seismic stability of high-rising buildings using grid-characteristic method. Procedia Comput Sci 2019;154:305–10. https://doi.org/10.1016/j.procs.2019.06.044.

[10] Keshavarz A, Mansoori Moghaddam B. Probabilistic seismic hazard analysis and determination of uniform hazard spectrum of Bushehr province assuming linear source model. J Struct Constr Eng 2018;5:127–42. https://doi.org/10.22065/jsce.2017.86053.1181.

[11] Sunardi B, Rohadi S, Indriyani AD, Karnawati D. Re-Evaluation of Seismic Hazard in Tasikmalaya City Using Probabilistic Approach. GEOMATE J 2019;17:187–94. https://doi.org/10.21660/2019.63.60620.

[12] Alizadeh B, Pourzeynali S. Probabilistic Seismic Hazard Analysis Using the New Correlation Relationships for Magnitude Scales. Civ Eng J 2018;4:872–85. https://doi.org/10.21660/2019.63.60620.

[13] Ghodrati Amiri G, Razavian Amrei SA, Tahmasbi Broujeni MA. Seismic Hazard Analysis and Uniform Hazard Spectra for Different Regions of Kerman. J Struct Constr Eng 2015;2:43–51.

[14] Bakhshipour Sedaposhte A, Fahimi Farzam M. An Overview of the Concepts Earthquake and Applications of Seismic Risk Analysis and the Introduction of Methodology PSHA and DSHA. Road 2018;26:87–104.

[15] Zare M, Hashemi SA, Rahmani R. Seismic Hazard Analysis and Developping the Acceleration Zoning Maps in the Khark Island, Persian Gulf Iran. J Nat Environ Hazards 2015;4:1–12. https://doi.org/10.22111/jneh.2015.2471.

[16] Dastjerdi, H. D., Bakhshi, H., & Sadeghi M. Deterministic and Probabilistic Seismic Hazard Analysis of Petroleum Product Storage Facilities in Bushehr City. Earthq Eng J 2018;10(2):17–34.

[17] NEA/CSNI/R(2019)1. Comparison of Probabilistic Seismic Hazard Analysis of Nuclear Power Plants in Areas with Different Levels of Seismic Activity. 2019.

[18] Peñarubia HC, Johnson KL, Styron RH, Bacolcol TC, Sevilla WIG, Perez JS, et al. Probabilistic seismic hazard analysis model for the Philippines. Earthq Spectra 2020;36:44–68. https://doi.org/10.1177/8755293019900.

[19] ShamsAldane I NM. Earthquake Risk Analysis by determining and probabilistic Method and determining the acceleration and magnitude of the main faults caused by earthquake. Proc 18th Iran Geophusical Conf 2018.

[20] Bakhshi H, Rezaie Z. Preparation of same acceleration maps for use in the improvement of structures in Sabzevar city. J Rehabil Civ Eng 2021;9:101–19. https://doi.org/10.22075/jrce.2021.19219.1363.

[21] Ezzodin A, Ghodrati Amiri G, Raissi Dehkordi M. A random vibration-based simulation model for nonlinear seismic assessment of steel structures subjected to fling-step ground motion records. J Vib Eng Technol 2022;10:2641–55. https://doi.org/10.1007/s42417-022-00509-9.

[22] Sharafi SQ, Maulana TI, Saito T. Development and Validation of a Seismic Index for Assessing the Vulnerability of Low-Rise RC Buildings. Civ Eng J 2025;11. https://doi.org/10.28991/CEJ-2025-011-03-016.

[23] Nowroozi AA. Empirical relations between magnitudes and fault parameters for earthquakes in Iran. Bull Seismol Soc Am 1985;75:1327–38. https://doi.org/10.1785/BSSA0750051327.

[24] Ambraseys NN, Melville CP. A history of Persian earthquakes. Cambridge university press; 2005.

[25] Wells DL, Coppersmith KJ. New empirical relationships among magnitude, rupture length, rupture width, rupture area, and surface displacement. Bull Seismol Soc Am 1994;84:974–1002. https://doi.org/10.1785/BSSA0840040974.

[26] Gutenberg B, Richter CF. Frequency of earthquakes in California. Bull Seismol Soc Am 1944;34:185–8. https://doi.org/10.1785/BSSA0340040185.

[27] Bozorgnia Y, Abrahamson NA, Atik L Al, Ancheta TD, Atkinson GM, Baker JW, et al. NGA-West2 research project. Earthq Spectra 2014;30:973–87.

[28] McGuire RK. Seismic hazard and risk analysis. Seismol Soc Am 2004. https://doi.org/10.1785/gssrl.77.1.43.

[29] Bender B, Perkins DM. SEISRISK III: a computer program for seismic hazard estimation. US Government Printing Office; 1987.

[30] No S. 2800 (2015) of Iranian Code of Practice for Seismic Resistance Design of Buildings 2015.

[31] Minimum design loads and associated criteria for buildings and other structures. 2017. https://doi.org/10.1061/9780784414248.

[32] Code P. Eurocode 8: Design of structures for earthquake resistance-part 1: general rules, seismic actions and rules for buildings. Brussels Eur Comm Stand 2005;10.

[33] Survey USGS and CG. Quaternary fault and fold database for the United States 2018.

[34] ISC Bulletin. Int Seismol Cent n.d.

[35] Advanced National Seismic System (ANSS) Composite Earthquake Catalog. US Geol Surv n.d.

[36] Boore DM, Joyner WB. Site amplifications for generic rock sites. Bull Seismol Soc Am 1997;87:327–41. https://doi.org/10.1785/BSSA0870020327.

[37] Bakhshi H, Rakhshani Mehr M, Norouzi M. Seismic risk analysis and mapping acceleration Nishapur city. J Model Eng 2017;15:211–23. https://doi.org/10.22075/jme.2017.2562.

[38] Milad D MM. Seismic Hazard Analysis Of Busher City under the Movement of two High-Risk Faults in the region by tow methods: Deterministic and Probablistic. Natl Conf Fundam Reserach Civ Eng Archit Urban Dev 2018.

[39] Zhao, J., Campbell, K. W., & Chiou BS-J. NGA-West2 ground-motion prediction equations for the horizontal component of peak ground acceleration and spectral acceleration. Earthq Spectra 2016:369–387.

[40] Iman A MN-B. Providing relationships for the production of artificial acceleration mapping in the Iranian plateau with a random approach. J Earthq Sci Eng 2015.

[41] Briassoulis H. Analysis of land use change: theoretical and modeling approaches 2020.

[42] Kuehn NM, Abrahamson NA. Spatial correlations of ground motion for non-ergodic seismic hazard analysis. Earthq Eng Struct Dyn 2020;49:4–23.